Heliyon 10 (2024) e35439

Contents lists available at ScienceDirect

Heliyon

journal homepage: www.cell.com/heliyon

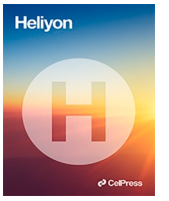

Research article

Exploring urinary proteomics and peptidomics biomarkers for the diagnosis of mekong schistosomiasis

Tipparat Thiangtrongjit [a], Poom Adisakwattana [b], Yanin Limpanont [c], Wang Nguitragool [a], Phiraphol Chusongsang [c], Yupa Chusongsang [c], Nuttapohn Kiangkoo [c], Onrapak Reamtong [a,*]

[a] Department of Molecular Tropical Medicine and Genetics, Faculty of Tropical Medicine, Mahidol University, Bangkok, Thailand
[b] Department of Helminthology, Faculty of Tropical Medicine, Mahidol University, Bangkok, Thailand
[c] Department of Social and Environmental Medicine, Faculty of Tropical Medicine, Mahidol University, Bangkok, Thailand

ARTICLE INFO

Keywords:
Schistosoma mekongi
Proteomics
Peptidomics
Biomarker

ABSTRACT

Schistosomiasis caused by *Schistosoma mekongi* is one of the causative agents of human blood fluke infection in the lower Mekong River. Traditionally, the detection of egg morphology in stool samples has served as the prevailing method for diagnosing *Schistosoma* infection. Nonetheless, this approach exhibits low sensitivity, particularly in early infection detection. Urine has been extensively studied as a noninvasive clinical sample for diagnosing infectious diseases. Despite this, urine proteomic analysis of *S. mekongi* infection has been less investigated. This study aimed to characterize proteins and peptides present in mouse urine infected with *S. mekongi* both before infection and at intervals of 1, 2, 4, and 8 weeks post-infection using mass spectrometry-based proteomics. Proteomics analysis revealed 13 up- and only one down-regulated mouse protein consistently found across all time points. Additionally, two *S. mekongi* uncharacterized proteins were detected throughout the infection period. Using a peptidomics approach, we consistently identified two peptide sequences corresponding to *S. mekongi* collagen alpha-1(V) in mouse urine across all time points. These findings highlight the potential of these unique proteins, particularly the *S. mekongi* uncharacterized proteins and collagen alpha-1(V), as potential biomarkers for early detection of *S. mekongi* infection. Such insights could significantly advance diagnostic strategies for human Mekong schistosomiasis.

1. Introduction

Schistosomiasis is a neglected tropical disease caused by blood flukes of the genus *Schistosoma*. This disease remains one of the most serious parasitic diseases, causing chronic human illness with serious consequences for socioeconomic development in tropical countries [1]. It is a widely distributed trematode infection in tropical regions with an estimated over 200 million people worldwide [2]. In Africa and South America, human schistosomiasis is caused mainly by *Schistosoma mansoni*, *S. haematobium,* and *S. intercalatum*, whereas *S. japonicum* and *S. mekongi* are the most common causative agents of intestinal schistosomiasis in Asia. *S. mekongi* affects communities in the Mekong River Basin, particularly in the southern Lao People's Democratic Republic (Lao PDR) and in northern Cambodia [3]. At present, an estimated 140,000 people are still at risk of *S. mekongi* infection; 80,000 in Cambodia and 60,000 in Laos

* Corresponding author.
E-mail address: onrapak.rea@mahidol.ac.th (O. Reamtong).

https://doi.org/10.1016/j.heliyon.2024.e35439
Received 19 April 2024; Received in revised form 26 July 2024; Accepted 29 July 2024
Available online 30 July 2024

[4].

Severe hypersensitivities such as acute Katayama syndrome and chronic granulomatous diseases are the main pathogenicity of schistosomiasis. The patients can have fever, malaise, myalgia, headache, eosinophilia, fatigue, and abdominal pain lasting 2–10 weeks. The systemic hypersensitivity reaction occurs during the migrating schistosomula stage, worm maturation, egg production, and the release of egg antigens [5]. The parasite eggs trapped in the host organs and tissues cause the granulomatous inflammatory reaction that causes chronic schistosomiasis [2]. Accurate diagnostic methods are the first step in eliminating schistosomiasis and reducing morbidity [5]. The Kato–Katz method is commonly used to detect *S. mekongi* eggs based on the egg morphology in stool samples using microscopy. However, this method is insensitive when patients have a light infection with low egg intensity [6]. An immunochromatographic test (ICT) based on anti-schistosomal antibody detection in human sera has been developed using somatic antigens from adult *S. mekongi* [7]. Schistosome-specific antigens have been evaluated using *S. mansoni* antigens [8], and crude antigen and recombinant antigens of *S. japonicum* to detect *S. mekongi*-directed antibodies in human serum [9]. Immunodiagnostic techniques are sensitive, easy to perform, and useful as epidemiological tools for screening targeted populations in schistosome-endemic areas [10]. Serological assays for detecting anti-schistosome specific antibodies are beneficial for travelers, migrants, and individuals in low-transmission areas. However, this technique may show cross-reactivity with other helminth infections, and the assay results can remain positive for several years after treatment [2]. The circulating anodic antigens (CAAs) and circulating cathodic antigens (CCAs) are proteoglycans that can be identified in urine using enzyme-linked immunosorbent assay (ELISA) or monoclonal antibody-based lateral flow tests. Detection of CAA and CCA indicates active infection in the presence of worms before egg production begins [5]. The antigen test offers higher specificity and can differentiate between active and past infections. Unlike other schistosome species, there are currently no CAA- or CCA-based ELISA or lateral flow tests available for detecting *S. mekongi*. Molecular methods based on polymerase chain reaction (PCR) have been developed to differentiate and identify *S. mekongi* from the major important human schistosomes including *S. mansoni*, *S. haematobium*, *S. japonicum* [11]. A real-time PCR assay combined with melting-curve analysis has been developed for detecting *S. mekongi* DNA in infected snails and rat feces [12]. PCR is more sensitive than microscopic egg detection [13]. However, the use of stool or urine samples for molecular techniques is limited due to inhibitors present in the samples [14]. PCR-based methods are costly, require skilled personnel, and are not practical in field settings [1]. Improvements in diagnostic methods are necessary to enhance the precision of schistosomiasis diagnosis and reduce morbidity. The selection of specific biomarkers is crucial for diagnosing various phases of infection, including acute and chronic phases, as well as post-treatment stages [15].

Proteomic analysis is a high-throughput technology that analyzes protein expression using gel- or non-gel-based protein separation techniques, coupled with mass spectrometry and bioinformatics [16]. Protein identification from biological samples including tissue, blood, urine, and stool can provide biomarkers for the detection and development of the disease, guiding targeted treatment [17]. Urine serves as a biological fluid for identifying novel biomarkers that could potentially aid in diagnosis. The non-invasive procedure is generally painless and low risk for patients undergoing diagnosis [18]. Proteomics has been applied to identify schistosome proteins from complex samples including the egg protein of *S. mekongi* [19] and somatic and excretory-secretory proteins of adult *S. mekongi* [20].

This study aimed to identify a candidate protein biomarker for early detection of *S. mekongi* in urine samples utilizing a mouse model of schistosomiasis. Urine samples collected before infection and at various timepoints (1, 2, 4, and 8 weeks post-infection) were analyzed by gel electrophoresis coupled with mass spectrometry (LC-MS/MS). These findings provide new candidate biomarkers in urine samples for protein-based diagnosis of early *S. mekongi* infection.

2. Materials and methods

2.1. Preparation of infected mouse

All animal experiments were approved by the Faculty of Tropical Medicine Animal Care and Use Committee (FTM-ACUC), Mahidol University (FTM-ACUC 017/2022). Mice experimentally infected with *S. mekongi*, were maintained in the Animal Care Unit, Faculty of Tropical Medicine, Mahidol University. Eight-week-old female ICR mice (3 mice) had their abdomen area shaved and were infected by 30 cercariae of *S. mekongi* using a hairpin loop. Urine was collected at 1, 2, 4, and 8 weeks post-infection. The urine samples were kept at −80 °C until use.

2.2. Protein separation from mouse urine

The urine samples were thawed on ice and centrifuged at 1000 g for 30 min at 4 °C. The supernatants were collected, and the protein concentration in the urine supernatants was determined using the Bradford method. The average concentration was 4.17 mg/ml. According to the protein concentration measured by Bradford, the volumes of urine containing thirty μg of protein were dissolved in 2x Laemmli Sample Buffer (BIO-RAD, CA, USA) and loaded onto gel electrophoresis. The urine proteins were separated using 12 % SDS-PAGE. The gel was stained with Coomassie Brilliant Blue R250. All gel bands were excised into 12 pieces in each lane and processed for in-gel tryptic digestion.

2.3. In-gel tryptic digestion

Proteins within each gel piece were destained with 50 % acetonitrile in 50 mM ammonium bicarbonate until colorless. The gel pieces were reduced by 4 mM dithiothreitol at 60 °C for 45 min. After reduction, the gel pieces were alkylated with 250 mM

iodoacetamide at room temperature in the dark for 30 min, and the reaction was quenched by adding 4 mM dithiothreitol at room temperature for 5 min. Gel pieces were dehydrated by adding 100 % acetonitrile. The supernatant was removed. Gel pieces were rehydrated by adding 10 ng/ul trypsin (Sigma-aldrich, USA) in 50 mM ammonium bicarbonate followed by 50 mM ammonium bicarbonate containing 5 % acetonitrile. The solution was incubated at 37 °C overnight. The peptides were extracted by adding acetonitrile and incubating at room temperature for 20 min. The peptide solution was transferred to a new microcentrifuge tube and dried by using a centrifuge concentrator (Tomy, Japan).

2.4. Peptide preparation

The urine samples were centrifuged at 1000 g for 30 min at 4 °C. The urine supernatants were filtered using Amicon Ultra 0.5 mL with 30 kDa molecular weight cutoff (Millipore, Germany), centrifuged at 15,000×*g*, 4 °C for 20 min. Peptides in the samples were desalted and enriched using C18 ZipTips (Millipore, Germany). The tips were rinsed with 50 % acetonitrile and then equilibrated with 0.1 % trifluoroacetic acid (TFA). The samples were washed with 0.1 % TFA and eluted in 5 μl of 80 % acetonitrile, 0.1 % TFA solution. The peptide solution was dried by using a centrifuge concentrator (Tomy, Japan).

2.5. Mass spectrometric analysis

The peptide was resuspended with 0.1 % formic acid and injected into a nano-liquid chromatography system (Dionex Ultimate 3000, Surrey, UK). The peptide mixture was loaded onto the Acclaim PepMap RSLC 75 μm × 15 cm nanoviper C18 with a 2 μm particle size and a 100 A° pore size (Thermo Scientific, Waltham, USA). The nanoflow LC system was coupled with a MicroTof Q II mass spectrometer (Bruker; Bremen, Germany). Mass spectrometer data covered *m/z* ranges of 500–3500 *m/z*.

The MS/MS spectra were analyzed with data analysis software (Bruker Daltonics), converted to mgf files, and searched against the mouse database using the MASCOT search engine 2.3 (Matrix Science, Chicago, USA) with the following parameter settings: trypsin digestion; one missed cleavage; variable modifications of carbamidomethyl (C) and oxidation (M). Peptide tolerance was 0.8 Da, and fragment mass tolerance was ±0.8 Da.

To identify the proteins and peptides of *S. mekongi* in the urine sample, we used an in-house *S. mekongi* transcriptomic database. Detailed information about the *S. mekongi* transcriptome can be found in the study by Phuphisut O et al., 2018 [21]. The protein

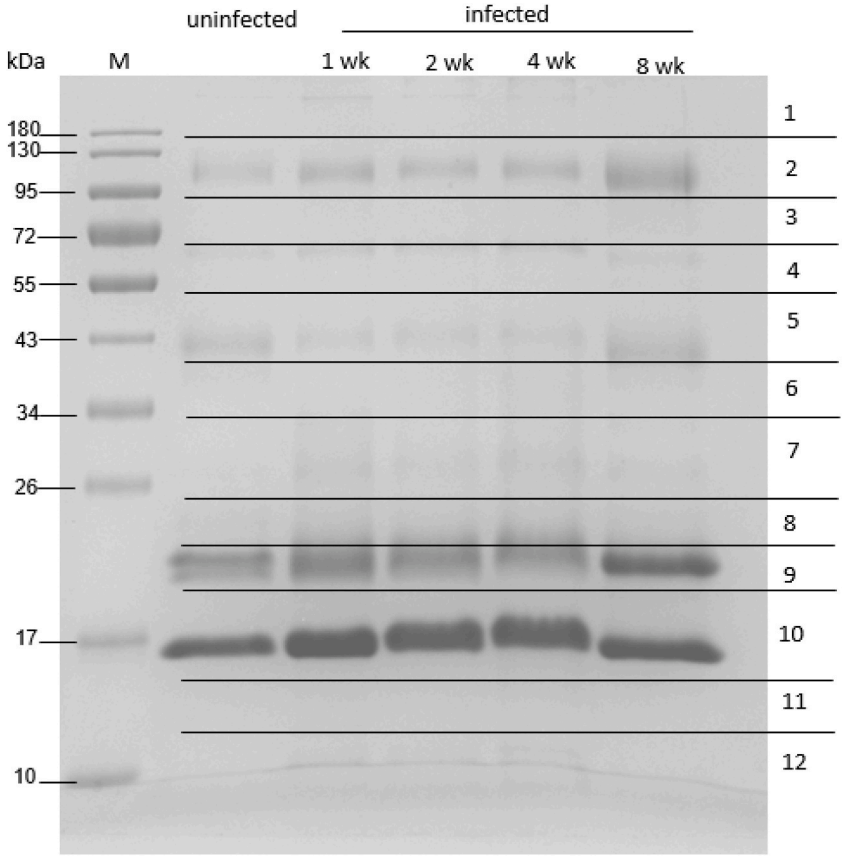

Fig. 1. SDS-PAGE analysis of *S. mekongi* infected mouse urine before (uninfected) and at 1, 2, 4, and 8 weeks after infection.

abundance was performed semi-quantitatively using the exponentially modified protein abundance index (emPAI) [22].

To identify mouse serum protein differentiation, the UniProt database was used for analysis, and the organism was set as *Mus musculus*. The statistical analysis was performed using the Perseus software platform (https://maxquant.net/perseus/). A fold change cutoff of 2 was applied for both upregulated and downregulated proteins, and a *t*-test was used to determine significance at $p < 0.05$. Principal component analysis (PCA) and partial least squares discriminant analysis (PLS-DA) were analyzed using MetaboAnalyst 6.0. Protein-protein interaction of up-regulated mouse urine proteins was analyzed using the String database. Gene ontology was assigned using the Uniprot database.

2.6. Bioinformatic analysis

The protein sequence of the *S. mekongi* accession no Gene.25154 and Gene. 22949 were retrieved from the nonredundant protein database of the National Center for Biotechnology Information (NCBI). The protein sequences of *S. mansoni*, *S. japonicum*, *Mus musculus,* and *Homo sapiens* were obtained from the nonredundant protein database of NCBI. The sequences of identified proteins were submitted to a BLAST server (http://www.ncbi.nlm.nih.gov/BLAST/) to find similar sequences. All sequence alignments and calculations of percent identity were performed using the Clustal Omega software.

The peptide sequences of the *S. mekongi* were retrieved from an in-house transcriptome database. The protein sequence of *S. mekongi*, *S. mansoni*, *S. japonicum*, *Mus musculus,* and *Homo sapiens* were obtained from the nonredundant protein database of NCBI. Sequences of identified proteins were submitted to a BLAST server (http://www.ncbi.nlm.nih.gov/BLAST/) to find similar sequences. All sequence alignments and calculations of percent identity were performed using the Clustal Omega software.

3. Results

3.1. Proteomic analysis of mouse urine infected with S. mekongi

Urine samples obtained from experimental mice infected with *S. mekongi* were subjected to SDS-PAGE separation (Fig. 1) followed by Mass spectrometry analysis to identify up-regulated and down-regulated mouse proteins in the urine at four timepoints relative to pre-infection. Volcano plots of mouse urine proteins quantification at 1, 2, 4, and 8 weeks post-infection relative to pre-infection determined by LC-MS/MS were provided in Supplemental Data 1. Principal component analysis (PCA) and partial least squares discriminant analysis (PLS-DA) were performed for feature extraction and discriminant analysis between uninfected and infected mice (Fig. 2A and B). Uninfected mouse samples clustered separately from infected mouse samples. PLS-DA provided better sample differentiation. Throughout the time course, the number of up-regulated proteins was higher than the down-regulated proteins. Twenty, twenty-five, twenty-four, and thirty-seven mouse proteins were up-regulated at 1, 2 4, and 8 weeks respectively, whereas only one mouse protein was down-regulated at each time point (Table 1, Table 2).

The up-regulated mouse urine proteins at 1, 2, 4, and 8 weeks post-infection were analyzed for their protein-protein interaction (Supplemental Data 2). The results indicated that structural molecule activity (GO:0005198) and negative regulation of insulin secretion involved in the cellular response to glucose stimulus (GO:0061179) were observed at 1, 2, and 4 weeks post-infection. At 8 weeks post-infection, in addition to the interactions found earlier, acute phase response (KW-0011) and complement alternate pathway

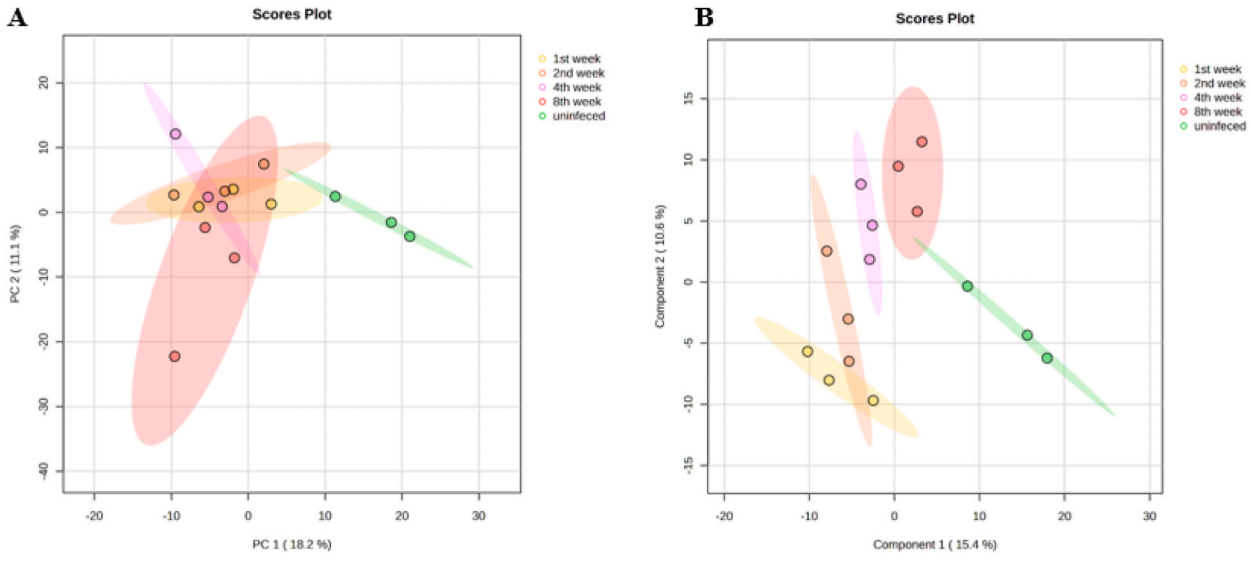

Fig. 2. Clustering mouse urine samples based on protein expression with (A) Principal component analysis (PCA) and (B) Partial least squares discriminant analysis (PLS-DA). Samples from three mice before (uninfected) and at 1, 2, 4, and 8 weeks after infection were included.

Table 1
Mouse proteins up-regulated at 1, 2, 4, and 8 weeks post-infection relative to pre-infection, as determined by LC-MS/MS.

Week	No	Accession no	Protein	Score	M.W.	No. of peptide	% Coverage	pI	-LOG (P-value)	LOG2FC
1st	1	MUP2_MOUSE	Major urinary protein 2	7163	20650	19	97.8	5.04	3.54	5.55
	2	MUP6_MOUSE	Major urinary protein 6	5279	20636	17	97.8	4.89	3.75	5.07
	3	MUP1_MOUSE	Major urinary protein 1	5142	20635	17	97.8	5.02	3.88	4.92
	4	MUP3_MOUSE	Major urinary protein 3	3055	21451	14	66.8	4.8	3.03	4.64
	5	UROM_MOUSE	Uromodulin	2471	70798	23	38.5	4.75	3.01	3.90
	6	CFAD_MOUSE	Complement factor D	3019	28039	10	49.8	6.18	3.46	3.40
	7	ALBU_MOUSE	Serum albumin	1704	68648	35	59	5.75	2.17	3.37
	8	KLK1_MOUSE	Kallikrein-1	412	28756	9	40.2	4.96	3.35	3.05
	9	EGF_MOUSE	Pro-epidermal growth factor	1619	133058	30	29.6	6.05	2.33	2.66
	10	K1B11_MOUSE	Kallikrein 1-related peptidase b11	128	28708	5	23.4	6.69	3.52	2.10
	11	K1C24_MOUSE	Keratin, type I cytoskeletal 24	301	54007	7	18.6	4.93	2.71	2.10
	12	K22E_MOUSE	Keratin, type II cytoskeletal 2 epidermal	1162	70880	12	21.9	8.26	2.52	1.83
	13	KT33B_MOUSE	Keratin, type I cuticular Ha3-II	296	45834	6	20.8	4.79	1.49	1.53
	14	FA2H_MOUSE	Fatty acid 2-hydroxylase	30	42954	4	14	6.76	1.39	1.51
	15	K2C5_MOUSE	Keratin, type II cytoskeletal 5	720	61729	7	16.2	7.59	3.89	1.44
	16	TFDP1_MOUSE	Transcription factor Dp-1	34	45203	3	13.9	5.78	1.70	1.40
	17	KRT35_MOUSE	Keratin, type I cuticular Ha5	296	50497	7	20	4.9	1.65	1.36
	18	K1C17_MOUSE	Keratin, type I cytoskeletal 17	439	48132	7	26.1	5	1.31	1.29
	19	ZFY1_MOUSE	Zinc finger Y-chromosomal protein 1	23	88173	7	11.3	5.94	1.31	1.26
	20	CD166_MOUSE	CD166 antigen	28	65051	5	16.6	5.85	1.81	1.17
2nd	1	MUP2_MOUSE	Major urinary protein 2	7163	20650	19	97.8	5.04	4.19	5.65
	2	MUP6_MOUSE	Major urinary protein 6	5279	20636	17	97.8	4.89	4.93	5.20
	3	MUP1_MOUSE	Major urinary protein 1	5142	20635	17	97.8	5.02	5.78	4.93
	4	MUP3_MOUSE	Major urinary protein 3	3055	21451	14	66.8	4.8	3.23	4.73
	5	UROM_MOUSE	Uromodulin	2471	70798	23	38.5	4.75	2.99	3.61
	6	CFAD_MOUSE	Complement factor D	3019	28039	10	49.8	6.18	4.59	3.35
	7	ALBU_MOUSE	Serum albumin	1704	68648	35	59	5.75	1.64	2.95
	8	KLK1_MOUSE	Kallikrein-1	412	28756	9	40.2	4.96	2.41	2.64
	9	EGF_MOUSE	Pro-epidermal growth factor	1619	133058	30	29.6	6.05	2.48	2.59
	10	K2C1_MOUSE	Keratin, type II cytoskeletal 1	1430	65565	8	15.7	8.39	2.93	2.31
	11	K1C24_MOUSE	Keratin, type I cytoskeletal 24	301	54007	7	18.6	4.93	2.73	2.05
	12	FA2H_MOUSE	Fatty acid 2-hydroxylase	30	42954	4	14	6.76	3.80	1.95
	13	K1H1_MOUSE	Keratin, type I cuticular Ha1	296	47087	5	14.9	4.87	2.48	1.91
	14	K22E_MOUSE	Keratin, type II cytoskeletal 2 epidermal	1162	70880	12	21.9	8.26	2.53	1.79
	15	K2C79_MOUSE	Keratin, type II cytoskeletal 79	167	57517	9	16	7.55	3.03	1.69
	16	TMPS3_MOUSE	Transmembrane protease serine 3	31	49460	5	15.5	6.05	4.56	1.68
	17	K1C14_MOUSE	Keratin, type I cytoskeletal 14	363	52834	8	23.1	5.1	1.51	1.63
	18	K2C5_MOUSE	Keratin, type II cytoskeletal 5	720	61729	7	16.2	7.59	3.10	1.51
	19	KRT35_MOUSE	Keratin, type I cuticular Ha5	296	50497	7	20	4.9	2.35	1.47
	20	CD166_MOUSE	CD166 antigen	28	65051	5	16.6	5.85	3.06	1.44
	21	KT33B_MOUSE	Keratin, type I cuticular Ha3-II	296	45834	6	20.8	4.79	1.43	1.40
	22	DDX52_MOUSE	Probable ATP-dependent RNA helicase DDX52	20	67400	4	9.9	9.57	1.62	1.38
	23	K1C28_MOUSE	Keratin, type I cytoskeletal 28	261	50315	4	10.6	5.19	1.61	1.33
	24	ABCB7_MOUSE	ATP-binding cassette sub-family B member 7, mitochondrial	30	82543	4	5.9	9.36	1.60	1.20
	25	ASAP2_MOUSE	Arf-GAP with SH3 domain, ANK repeat, and PH domain-containing protein 2	52	106738	8	15.2	6.22	1.71	1.06
4th	1	MUP2_MOUSE	Major urinary protein 2	7163	20650	19	97.8	5.04	4.25	5.64
	2	MUP6_MOUSE	Major urinary protein 6	5279	20636	17	97.8	4.89	5.72	5.17
	3	MUP1_MOUSE	Major urinary protein 1	5142	20635	17	97.8	5.02	5.46	5.02
	4	MUP3_MOUSE	Major urinary protein 3	3055	21451	14	66.8	4.8	4.00	4.74
	5	ALBU_MOUSE	Serum albumin	1704	68648	35	59	5.75	3.50	3.94
	6	UROM_MOUSE	Uromodulin	2471	70798	23	38.5	4.75	3.66	3.52
	7	CFAD_MOUSE	Complement factor D	3019	28039	10	49.8	6.18	4.33	3.24
	8	KLK1_MOUSE	Kallikrein-1	412	28756	9	40.2	4.96	3.29	2.99
	9	GLCM1_MOUSE	Glycosylation-dependent cell adhesion molecule 1	245	16199	3	27.2	4.51	3.51	2.73
	10	K1C17_MOUSE	Keratin, type I cytoskeletal 17	439	48132	7	26.1	5	4.60	2.69
	11	K2C1_MOUSE	Keratin, type II cytoskeletal 1	1430	65565	8	15.7	8.39	4.19	2.69
	12	ECP1_MOUSE	Eosinophil cationic protein 1	370	17285	7	68.4	9.28	2.83	2.65
	13	K1C15_MOUSE	Keratin, type I cytoskeletal 15	475	49107	8	27.7	4.79	3.75	2.57
	14	K1C13_MOUSE	Keratin, type I cytoskeletal 13	468	47724	8	21.7	4.79	3.63	2.55
	15	EGF_MOUSE	Pro-epidermal growth factor	1619	133058	30	29.6	6.05	3.41	2.45
	16	K1C19_MOUSE	Keratin, type I cytoskeletal 19	439	44515	8	16.4	5.28	4.56	2.38
	17	K1C10_MOUSE	Keratin, type I cytoskeletal 10	1110	57735	7	16.8	5.04	3.13	2.36

(*continued on next page*)

Table 1 (*continued*)

Week	No	Accession no	Protein	Score	M.W.	No. of peptide	% Coverage	pI	-LOG (P-value)	LOG2FC
	18	DNAS1_MOUSE	Deoxyribonuclease-1	122	32007	5	16.2	4.76	1.99	2.26
	19	K2C74_MOUSE	Keratin, type II cytoskeletal 74	783	54712	8	18.4	5.51	2.59	2.16
	20	K1C14_MOUSE	Keratin, type I cytoskeletal 14	363	52834	8	23.1	5.1	3.46	2.09
	21	K2C6A_MOUSE	Keratin, type II cytoskeletal 6A	733	59299	7	13.2	8.04	2.67	2.07
	22	K1C24_MOUSE	Keratin, type I cytoskeletal 24	301	54007	7	18.6	4.93	2.86	2.04
	23	THRB_MOUSE	Prothrombin	286	70224	10	20.7	6.04	3.40	1.95
	24	K1B21_MOUSE	Kallikrein 1-related peptidase b21	128	28671	4	21.8	7.05	2.39	1.91
	25	IBP5_MOUSE	Insulin-like growth factor-binding protein 5	34	30352	8	36.9	8.48	3.63	1.89
	26	K1B11_MOUSE	Kallikrein 1-related peptidase b11	128	28708	5	23.4	6.69	3.27	1.89
	27	K22E_MOUSE	Keratin, type II cytoskeletal 2 epidermal	1162	70880	12	21.9	8.26	2.65	1.84
	28	K1C18_MOUSE	Keratin, type I cytoskeletal 18	300	47509	8	22.9	5.22	2.00	1.74
	29	K1H1_MOUSE	Keratin, type I cuticular Ha1	296	47087	5	14.9	4.87	2.33	1.73
	30	KT33B_MOUSE	Keratin, type I cuticular Ha3-II	296	45834	6	20.8	4.79	2.66	1.69
	31	K2C75_MOUSE	Keratin, type II cytoskeletal 75	720	59704	6	13.2	8.46	2.59	1.69
	32	K2C79_MOUSE	Keratin, type II cytoskeletal 79	167	57517	9	16	7.55	2.79	1.65
	33	K2C5_MOUSE	Keratin, type II cytoskeletal 5	720	61729	7	16.2	7.59	3.05	1.62
	34	K2C71_MOUSE	Keratin, type II cytoskeletal 71	783	57347	6	13.4	6.6	2.56	1.62
	35	K2C8_MOUSE	Keratin, type II cytoskeletal 8	211	54531	7	15.5	5.7	2.82	1.59
	36	CF058_MOUSE	Uncharacterized protein C6orf58 homolog	332	38259	9	36.5	4.19	1.30	1.52
	37	KRT36_MOUSE	Keratin, type I cuticular Ha6	296	52757	7	18	4.99	2.06	1.50
	38	K22O_MOUSE	Keratin, type II cytoskeletal 2 oral	155	62806	8	13.6	8.68	1.85	1.48
	39	CADH1_MOUSE	Cadherin-1	238	98195	8	17	4.69	1.51	1.48
	40	KRT35_MOUSE	Keratin, type I cuticular Ha5	296	50497	7	20	4.9	2.65	1.48
	41	K1KB5_MOUSE	Kallikrein 1-related peptidase b5	52	28729	4	21.5	5.31	1.36	1.47
	42	ZFY2_MOUSE	Zinc finger Y-chromosomal protein 2	23	88071	5	8.8	5.89	1.56	1.32
	43	CATE_MOUSE	Cathepsin E	91	42905	4	11.6	4.49	2.89	1.18
	44	M3K8_MOUSE	Mitogen-activated protein kinase kinase kinase 8	47	52908	7	20.1	5.76	1.70	1.14
8th	1	MUP2_MOUSE	Major urinary protein 2	7163	20650	19	97.8	5.04	4.11	5.48
	2	MUP6_MOUSE	Major urinary protein 6	5279	20636	17	97.8	4.89	4.77	4.98
	3	MUP1_MOUSE	Major urinary protein 1	5142	20635	17	97.8	5.02	5.62	4.98
	4	MUP3_MOUSE	Major urinary protein 3	3055	21451	14	66.8	4.8	3.28	4.25
	5	ALBU_MOUSE	Serum albumin	1704	68648	35	59	5.75	3.27	3.97
	6	ECP1_MOUSE	Eosinophil cationic protein 1	370	17285	7	68.4	9.28	3.74	3.94
	7	UROM_MOUSE	Uromodulin	2471	70798	23	38.5	4.75	4.03	3.93
	8	AMBP_MOUSE	Protein AMBP	952	39004	16	39	5.96	3.62	3.38
	9	CFAD_MOUSE	Complement factor D	3019	28039	10	49.8	6.18	4.19	3.23
	10	KLK1_MOUSE	Kallikrein-1	412	28756	9	40.2	4.96	3.47	3.22
	11	HPT_MOUSE	Haptoglobin	595	38727	15	46.7	5.88	3.19	3.21
	12	PTGDS_MOUSE	Prostaglandin-H2 D-isomerase	141	21053	5	27.5	8.39	2.65	2.66
	13	CF058_MOUSE	Uncharacterized protein C6orf58 homolog	332	38259	9	36.5	4.19	3.34	2.62
	14	EGF_MOUSE	Pro-epidermal growth factor	1619	133058	30	29.6	6.05	3.06	2.48
	15	K2C1_MOUSE	Keratin, type II cytoskeletal 1	1430	65565	8	15.7	8.39	3.34	2.42
	16	K1C10_MOUSE	Keratin, type I cytoskeletal 10	1110	57735	7	16.8	5.04	2.85	2.39
	17	K2C74_MOUSE	Keratin, type II cytoskeletal 74	783	54712	8	18.4	5.51	2.63	1.99
	18	K1B21_MOUSE	Kallikrein 1-related peptidase b21	128	28671	4	21.8	7.05	2.47	1.99
	19	THRB_MOUSE	Prothrombin	286	70224	10	20.7	6.04	2.98	1.96
	20	K1B11_MOUSE	Kallikrein 1-related peptidase b11	128	28708	5	23.4	6.69	3.40	1.96
	21	NAPSA_MOUSE	Napsin-A	320	45516	3	11.7	7.14	2.23	1.94
	22	K1KB3_MOUSE	Kallikrein 1-related peptidase b3	131	28979	7	33.3	6.37	4.84	1.86
	23	K22E_MOUSE	Keratin, type II cytoskeletal 2 epidermal	1162	70880	12	21.9	8.26	2.68	1.83
	24	K2C73_MOUSE	Keratin, type II cytoskeletal 73	783	58875	9	21	8.36	2.82	1.81
	25	K1C24_MOUSE	Keratin, type I cytoskeletal 24	301	54007	7	18.6	4.93	2.43	1.80
	26	K2C79_MOUSE	Keratin, type II cytoskeletal 79	167	57517	9	16	7.55	3.02	1.58
	27	NEUR2_MOUSE	Sialidase-2	19	42376	3	7.1	7.65	1.57	1.54
	28	CFAB_MOUSE	Complement factor B	319	84951	7	13.7	7.18	2.80	1.48
	29	K2C75_MOUSE	Keratin, type II cytoskeletal 75	720	59704	6	13.2	8.46	2.57	1.48
	30	K2C71_MOUSE	Keratin, type II cytoskeletal 71	783	57347	6	13.4	6.6	2.76	1.44
	31	CD44_MOUSE	CD44 antigen	85	85565	5	9.4	4.82	2.67	1.37
	32	K22O_MOUSE	Keratin, type II cytoskeletal 2 oral	155	62806	8	13.6	8.68	2.01	1.30
	33	K2C5_MOUSE	Keratin, type II cytoskeletal 5	720	61729	7	16.2	7.59	3.57	1.29
	34	K2C1B_MOUSE	Keratin, type II cytoskeletal 1b	783	61322	7	16.3	7.74	2.21	1.29
	35	MEP1A_MOUSE	Meprin A subunit alpha	125	84143	9	20.1	5.81	2.97	1.24
	36	KRT35_MOUSE	Keratin, type I cuticular Ha5	296	50497	7	20	4.9	1.33	1.20
	37	K1C14_MOUSE	Keratin, type I cytoskeletal 14	363	52834	8	23.1	5.1	1.48	1.19

Table 2
Mouse proteins downregulated at 1, 2, 4, and 8 weeks post-infection relative to pre-infection, as determined by LC-MS/MS.

Week	No	Accession no	Protein	Score	M.W.	No. of peptide	% Coverage	pI	-LOG (P-value)	LOG2FC
1st	1	Q3U6A3	Monocyte differentiation antigen CD14	281	39145	4	18.6	5.08	2.56	−2.17
2nd	1	Q3U6A3	Monocyte differentiation antigen CD14	281	39145	4	18.6	5.08	2.40	−2.10
4th	1	Q3U6A3	Monocyte differentiation antigen CD14	281	39145	4	18.6	5.08	2.46	−1.91
8th	1	Q3U6A3	Monocyte differentiation antigen CD14	281	39145	4	18.6	5.08	2.26	−2.07

(KW-0179) were also detected. All mouse urine proteins exhibiting up-regulation were also used to construct a Venn diagram (Fig. 3). The common thirteen mouse proteins demonstrated up-regulation consistently at 1, 2, 4, and 8 weeks post-infection. These include keratin, type I cuticular Ha5; major urinary protein 2; keratin, type II cytoskeletal 5; keratin, type II cytoskeletal 2 epidermal; pro-epidermal growth factor; complement factor D; keratin, type I cytoskeletal 24; kallikrein-1; serum albumin; major urinary protein 6; major urinary protein 3; uromodulin and major urinary protein 1. Conversely, only one protein - monocyte differentiation antigen CD14 - was consistently down-regulated across all four infection timepoints (Table 3). These identified differentially expressed mouse proteins hold promise as potential diagnostic markers for Mekong schistosomiasis.

3.2. Proteomic analysis of S. mekongi proteins in mouse urine

Urine samples obtained from experimental mice infected with *S. mekongi* were determined by SDS-PAGE separation. Mass spectrometry analysis was performed to identify the proteins. All identified *S. mekongi* proteins are shown in Table 4 and S2. There were 11, 11, 8, and 18 *S. mekongi* proteins in infected mouse urine at the 1st, 2nd, 4th, and 8th weeks after infection. Among all *S. mekongi* proteins in urine, only two *S. meknogi* proteins were detected in all four infection time points (Fig. 4). The proteins were accession numbers as Gene 25154 and Gene 22949 and identified as uncharacterized proteins (Table 4). The alignment of these two proteins was conducted, comparing them with corresponding counterparts in the human and mouse proteomes, aiming to assess their potential candidacy as biomarkers for Mekong schistosomiasis.

3.3. Alignment of S. mekongi protein sequence

The sequence of *S. mekongi* uncharacterized protein (Gene.25154) was aligned with orthologs in other *Schistosoma* species including *S. mansoni* and *S. japonicum*. The protein was also aligned with the mouse (*Mus musculus*) and human (*Homo sapiens*) proteins. All sequences were provided in Supplemental Data 3. The sequence of *S. mekongi* uncharacterized protein (Gene.25154) showed stronger similarity to its orthologs in *S. mansoni* (52.1 %) and *S. japonicum* (81.6 %) than to its orthologs in mouse (27.4 %) and human (27.8 %) (Fig. 5).

Whereas the BlastP analysis revealed none of the hit of similarity between the *S. mekongi* uncharacterized protein (Gene.22949) to the human and mouse genomes. These observations together underscore the potential of the *S. mekongi* uncharacterized proteins (Gene.25154) and (Gene.22949) as promising biomarker candidates, given their divergence from the host proteins.

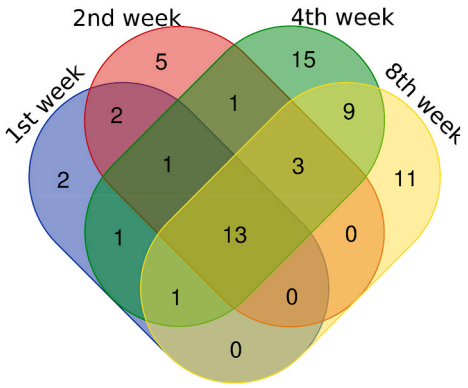

Fig. 3. Venn diagram of up-regulated proteins at 1, 2 4, and 8 weeks after infection.

Table 3
Mouse urine proteins up-regulated or down-regulated at all four timepoints of infection.

Regulation	No	Accession no	Protein	Gene ontology	Human ortholog
Up	1	KRT35_MOUSE	Keratin, type I cuticular Ha5	Structural molecule activity	Keratin 35
	2	MUP2_MOUSE	Major urinary protein 2	Glucose homeostasis	Lipocalin 9
	3	K2C5_MOUSE	Keratin, type II cytoskeletal 5	Structural molecule activity	Keratin 5
	4	K22E_MOUSE	Keratin, type II cytoskeletal 2 epidermal	Structural molecule activity	Keratin 75
	5	EGF_MOUSE	Pro-epidermal growth factor	Epithelial cell proliferation	Epidermal growth factor (beta-urogastrone)
	6	CFAD_MOUSE	Complement factor D	Response to bacterium	Complement factor D isoform 1
	7	K1C24_MOUSE	Keratin, type I cytoskeletal 24	Structural molecule activity	Keratin 24
	8	KLK1_MOUSE	Kallikrein-1	Regulation of systemic arterial blood pressure	Kallikrein
	9	ALBU_MOUSE	Serum albumin	Cellular response to starvation	Serum albumin
	10	MUP6_MOUSE	Major urinary protein 6	Glucose homeostasis	Lipocalin 9
	11	MUP3_MOUSE	Major urinary protein 3	Glucose homeostasis	Lipocalin 9
	12	UROM_MOUSE	Uromodulin	leukocyte cell-cell adhesion	Uromodulin
	13	MUP1_MOUSE	Major urinary protein 1	Glucose homeostasis	Lipocalin 9
Down	1	Q3U6A3	Monocyte differentiation antigen CD14	innate immune response	CD14 protein

3.4. Peptidomics analysis of S. mekongi in mouse urine by mass spectrometry

Peptides from infected mouse urine at 1, 2, 4, and 8 weeks were identified by mass spectrometry and searched against the in-house *S. mekongi* transcriptome. Among the identified *S. mekongi* peptides, only two peptides were found in all four timepoints. Peptides GLPGLPGLPGLPGHRGHKG and GLPGLPGLPGLPG were found in all four timepoints. The parent protein of these two peptides was collagen alpha-1(V) (Table 5).

The sequence of *S. mekongi* collagen alpha-1 protein was aligned with other *Schistosoma* species including *S. mansoni* and *S. japonicum*. The protein was also aligned with mouse (*Mus musculus*) and human (*Homo sapiens*) proteins. All sequences were provided in Supplemental Data 4. The sequence of *S. mekongi* collagen alpha-1 protein showed strong similarity to the sequence of *S. mansoni* (90.4 %) and *S. japonicum* (97.3 %). In addition, *S. mekongi* collagen alpha-1 protein demonstrated much lower percent similarity to mouse and human sequences (Fig. 6). Based on these findings, the collagen alpha-1 protein could be a viable candidate for the diagnosis of Mekong schistosomiasis.

4. Discussion

In this study, the use of only female mice may be considered a limitation. The mice were infected with *S. mekongi* cercariae at 7 weeks of age, with an average weight ranging from 26.3 to 31.3 g. After 8 weeks of infection, the weight of the infected mice ranged from 30.1 to 37.3 g, showing an increase in weight with age. Proteomic analysis of mouse urine before and after *S. mekongi* infection was performed using SDS-PAGE and mass-spectrometry. Urine is easy to collect, providing a noninvasive means to obtain a sample in large quantity and a valuable source for diagnostic biomarker discovery [23]. In our study, structural molecule activity (GO:0005198) and negative regulation of insulin secretion involved in the cellular response to glucose stimulus (GO:0061179) were up-regulated at 1, 2, and 4 weeks post-infection with *S. mekongi*. Cells of the immune system also express the insulin receptor and its downstream signaling components. The role of insulin signaling in controlling the immune response has been documented [24]. Therefore, the up-regulation of insulin signaling may be involved in the immune response following *S. mekongi* infection. Additionally, at 8 weeks post-infection, the acute phase response (KW-0011) and complement alternate pathway (KW-0179) were detected, indicating the activation of the mouse immune response to schistosome infection. Our analysis identified 13 up-regulated proteins at 1, 2 4, and 8 weeks in the urine after infection of mouse with *S. mekongi*. The major urinary protein (MUP) is a member family of lipocalin that is secreted in the circulation by the liver. MUP binds to lipophilic pheromones and regulates pheromone transportation and is excreted in urine. The function of circulating MUP is in metabolic glucose regulation and lipid metabolism [25]. The complement system is the first-line defense against invading pathogens. The human ortholog of MUP, lipocalin, is documented to be up-regulated in the uroepithelium and kidney of patients with urinary tract infections [26]. The up-regulation of MUPs could potentially be attributed to a host immune response, indicative of a defensive mechanism. Complement factor D is a 228-amino acid serine protease that circulates in a resting state at low plasma concentrations, primarily produced in adipocytes. Its main function is to cleave factor B, generating alternative pathway C3 convertases, making it a crucial and rate-limiting component in the alternative complement pathway amplification loop [27]. The complement system comprises a set of plasma proteins capable of activation either directly by pathogens or indirectly through pathogen-bound antibodies. This activation triggers a cascade of reactions occurring on the pathogen's surface, resulting in the generation of active components with diverse effector functions [28]. The up-regulation of complement factor D may be implicated in the host immune response to *S. mekongi* infection. Epidermal growth factor (EGF) is the prototypical member of a family of peptide growth factors that activate the EGF receptors. The EGF receptor signaling pathway plays an important role in the proliferation, differentiation, and migration of a variety of cell types, especially in epithelial cells [29]. Patients undergoing anti-cancer

therapy through the inhibition of the epidermal growth factor receptor (EGFR) were found to frequently experience skin infections attributed to *S. aureus*. The EGFR pathway plays a role in the induction of IL-1alpha and IL-1beta [30]. The observed up-regulation of EGF may be indicative of immune activation within the host organism. Kallikrein is a serine proteinase that produces the vasodilator kinin peptide from the kininogen substrate. The kallikrein–kinin system plays a role in the cardiovascular, renal, and central nervous systems [31]. This system maintains homeostasis of arterial pressure. The disturbance of this system may cause the pathogenesis of arterial high blood pressure and other cardiovascular disorders [32]. In *Trypanosoma cruzi* the proteolytic mechanisms governing the host/parasite equilibrium in peripheral sites of *T. cruzi* infection induced inflammatory edema and activated the kallikrein-kinin system, thereby promoting the stimulation of protective type-1 effector T cells [33]. The parasitic infection has the capability to activate the kallikrein-kinin system, thereby facilitating an immune response. The infection by *S. mekongi* may contribute to an

Table 4
The proteins of *S. mekongi* detected by LC-MS/MS in the urine samples from *S. mekongi* infected mice at 1, 2, 4, and 8-week timepoints. The red color denotes proteins that are consistently identified at all timepoints. The protein abundance represents in terms of the Exponentially modified protein abundance index (emPAI).

Week	No	Accession no.	Protein	Score	M.W.	%coverage	No. of peptide	pI	emPAI
1st	1	Gene.23354::comp7393_seq0::g.23354::m.23354	Uveal autoantigen with coiled-coil domains and ankyrin repeats protein, putative	35	210292	10	7.6	5.41	0.02
	2	Gene.735::comp157_seq0::g.735::m.735	Uncharacterized protein	28	250036	18	12.2	6.4	0.01
	3	Gene.2316::comp571_seq0::g.2316::m.2316	Clone ZZZ66 mRNA sequence	30	47539	4	10.9	6.3	0.14
	4	Gene.14035::comp4037_seq0::g.14035::m.14035	Uncharacterized protein	24	333480	15	7.6	8.52	0.01
	5	Gene.25154::comp8433_seq0::g.25154::m.25154	Uncharacterized protein	39	102028	3	4.4	6.45	0.03
	6	Gene.22923::comp7181_seq0::g.22923::m.22923	Neuronal differentiation protein	35	172143	10	8.6	8.74	0.02
	7	Gene.22949::comp7194_seq0::g.22949::m.22949	Uncharacterized protein	40	49907	3	8.2	8.95	0.07
	8	Gene.8302::comp2336_seq3::g.8302::m.8302	Uncharacterized protein	35	529397	26	7.8	5.65	0.01
	9	Gene.16778::comp4901_seq1::g.16778::m.16778	Uncharacterized protein	35	103136	6	8.1	9.34	0.03
	10	Gene.13382::comp3793_seq0::g.13382::m.13382	Ribosomal protein related	20	21642	4	29.1	9.72	0.16
	11	Gene.23768::comp7591_seq2::g.23768::m.23768	Uncharacterized protein	20	43440	2	7.6	8.35	0.08
2nd	1	Gene.2316::comp571_seq0::g.2316::m.2316	Clone ZZZ66 mRNA sequence	27	47539	5	15	6.3	0.07
	2	Gene.1037::comp250_seq0::g.1037::m.1037	Clone ZZZ332 mRNA sequence (Splicing factor, arginine/serine-rich 7)	28	19043	4	26.6	10.73	0.18
	3	Gene.21570::comp6626_seq2::g.21570::m.21570	Putative ATP-dependent RNA helicase DDX56	29	50280	2	6.4	9.84	0.07
	4	Gene.12046::comp3400_seq0::g.12046::m.12046	Putative ATPase	22	66034	3	6.9	9.1	0.05
	5	Gene.33801::comp84458_seq0::g.33801::m.33801	Histone H2A	47	10935	2	22	10.77	0.31
	6	Gene.25154::comp8433_seq0::g.25154::m.25154	Uncharacterized protein	30	102028	5	7.1	6.45	0.03
	7	Gene.27567::comp10875_seq1::g.27567::m.27567	Uncharacterized protein	20	83163	5	6	7	0.08
	8	Gene.7888::comp2206_seq1::g.7888::m.7888	SJCHGC06271 protein	24	25297	2	13.1	5.83	0.13
	9	Gene.25466::comp8663_seq0::g.25466::m.25466	Uncharacterized protein	37	39835	4	19.8	5.33	0.08
	10	Gene.22949::comp7194_seq0::g.22949::m.22949	Uncharacterized protein	23	49907	2	4.5	8.95	0.07
	11	Gene.22539::comp7018_seq0::g.22539::m.22539	Dock-9, putative	18	356867	15	7.5	7.28	0.01

4th	1	Gene.25154::comp8433_seq0::g.25154::m.25154	Uncharacterized protein	34	102028	4	5.8	6.45	0.03
	2	Gene.391::comp63_seq0::g.391::m.391	Ribosomal protein L26 (SJCHGC01959 protein)	18	16669	3	14.1	10.74	0.2
	3	Gene.22949::comp7194_seq0::g.22949::m.22949	Uncharacterized protein	35	49907	3	6.7	8.95	0.07
	4	Gene.12019::comp3392_seq1::g.12019::m.12019	Nicalin (M28 family)	20	73923	3	6.3	7.38	0.04
	5	Gene.12046::comp3400_seq0::g.12046::m.12046	Putative ATPase	27	66034	4	12.9	9.1	0.05
	6	Gene.23354::comp7393_seq0::g.23354::m.23354	Uveal autoantigen with coiled-coil domains and ankyrin repeats protein, putative	41	210292	9	7.8	5.41	0.02
	7	Gene.23768::comp7591_seq2::g.23768::m.23768	Uncharacterized protein	23	43440	5	22	8.35	0.08
	8	Gene.7597::comp2116_seq0::g.7597::m.7597	Clone ZZD1582 mRNA sequence	31	25608	3	11.7	8.78	0.13
8th	1	Gene.22949::comp7194_seq0::g.22949::m.22949	Uncharacterized protein	30	49907	4	10.9	8.95	0.07
	2	Gene.19029::comp5636_seq1::g.19029::m.19029	Putative 6-phosphofructo-2-kinase/fructose-2,6-bisphosph at ase	20	53500	5	11.6	8.59	0.06
	3	Gene.13382::comp3793_seq0::g.13382::m.13382	Ribosomal protein related	23	21642	3	19.8	9.72	0.16
	4	Gene.2316::comp571_seq0::g.2316::m.2316	Clone ZZZ66 mRNA sequence	19	47539	6	18.5	6.3	0.07
	5	Gene.17942::comp5288_seq2::g.17942::m.17942	Coiled-coil domain-containing protein 146	29	110511	9	11.1	8.76	0.03
	6	Gene.8744::comp2479_seq0::g.8744::m.8744	Neurobeachin	22	315602	12	6.5	6.01	0.01
	7	Gene.23768::comp7591_seq2::g.23768::m.23768	Uncharacterized protein	22	43440	3	8.4	8.35	0.08
	8	Gene.14062::comp4037_seq6::g.14062::m.14062	Uncharacterized protein	20	290007	14	6.1	8.5	0.01
	9	Gene.22539::comp7018_seq0::g.22539::m.22539	Dock-9, putative	36	356867	18	8	7.28	0.01
	10	Gene.8754::comp2479_seq3::g.8754::m.8754	Neurobeachin	22	266441	9	5.1	5.9	0.01
	11	Gene.18976::comp5618_seq2::g.18976::m.18976	Uncharacterized protein	23	24552	4	20	5.43	0.14
	12	Gene.1037::comp250_seq0::g.1037::m.1037	Clone ZZZ332 mRNA sequence (Splicing factor, arginine/serine-rich 7)	20	19043	4	27.8	10.73	0.18
	13	Gene.20591::comp6211_seq4::g.20591::m.20591	Rap guanine nucleotide exchange factor 2	24	108057	6	8.3	6.62	0.03
	14	Gene.23354::comp7393_seq0::g.23354::m.23354	Uveal autoantigen with coiled-coil domains and ankyrin repeats protein, putative	35	210292	8	6.5	5.41	0.02
	15	Gene.25154::comp8433_seq0::g.25154::m.25154	Uncharacterized protein	34	102028	4	7.7	6.45	0.03
	16	Gene.20585::comp6211_seq1::g.20585::m.20585	Rap guanine nucleotide exchange factor 2	24	267639	8	5.2	8.31	0.01
	17	Gene.391::comp63_seq0::g.391::m.391	Ribosomal protein L26 (SJCHGC01959 protein)	20	16669	1	7	10.74	0.2
	18	Gene.32669::comp47839_seq0::g.32669::m.32669	unknown	17	13078	2	22	10.17	0.26

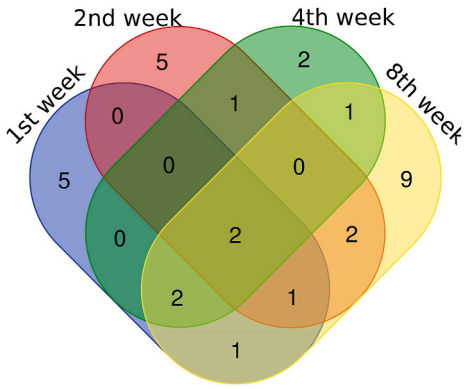

Fig. 4. Venn diagram of identified *S. mekongi* proteins in mouse urine at 1, 2 4, and 8 weeks after infection.

	Homo sapiens	*Mus musculus*	*S. mansoni*	*S. mekongi*	*S. japonicum*
Homo sapiens	100.0	61.0	24.4	27.8	28.0
Mus musculus	61.0	100.0	24.9	27.4	26.0
S. mansoni	24.4	24.9	100.0	52.1	53.0
S. mekongi	27.8	27.4	52.1	100.0	81.6
S. japonicum	28.0	26.0	53.0	81.6	100.0

Fig. 5. Percent identity matrix of *S. mekongi* uncharacterized protein (Gene.25154) in *S. mansoni*, *S. japonicum*, mouse, and human.

elevated expression of Kallikrein, consequently promoting mouse immune responses. Uromodulin is a glycoprotein, produced and secreted by tubular epithelial cells. The highly expressed uromodulin is related to kidney development and urinary tract obstruction leads to leukocyte recruitment and inflammatory kidney diseases [34]. The observed augmentation in urinary uromodulin levels may be indicative of a host immune response. Serum albumin is a common protein found in serum. In Brazil, an estimated 1.5 million individuals are afflicted with *S. mansoni* infection, and up to 15 % of diagnosed cases progress to renal impairment. Renal involvement in schistosomiasis is characterized by high-incidence glomerular lesions, particularly prevalent in chronically infected individuals residing in regions of elevated endemicity. Urinary creatinine and albumin were observed in *S. mansoni* infection resulting from kidney injury [35]. Nevertheless, the literature addressing schistosomiasis was correlated with urinary albumin as a biomarker of kidney injury. The down-regulated monocyte differentiation antigen CD14 was found in mouse urine at 1, 2, 4, and 8 weeks after infection The monocyte differentiation antigen CD14 is a pattern recognition receptor (PRR) that enhances innate immune responses against bacterial infection [36]. In humans, monocyte antigen CD14 was found in normal controls [37]. The major secretory product derived from *S. mansoni* eggs induces the release of IL-4/IL-13 from basophils, thereby inhibiting the release of inflammatory cytokines from human monocytes. These observations underscore the pivotal role of egg antigens in mediating the regulatory influence exerted by schistosomes on host inflammation [38]. The downregulation of the monocyte differentiation antigen CD14 could potentially indicate the *Schistosoma* parasite's suppression of host immunity. Due to the differential expression of mouse proteins identified in the urine of *S. mekongi* infected mice, a substantial proportion of these proteins are implicated in host immunity and contribute to the pathological response after infection. The differential observed in mouse proteins holds potential as biomarkers for diagnosing Mekong schistosomiasis. Nevertheless, it is essential to acknowledge that these alterations may lack specificity exclusive to *Schistosoma* infection, as similar protein differentials could manifest in response to infections by other pathogens. Consequently, these mouse proteins could serve as valuable supplementary diagnostic information when integrated with other diagnostic techniques. The identification *S. mekongi* proteins and peptides in urine could be more specific for schistosomiasis diagnosis. For *S. mekongi* protein identification, uncharacterized proteins (Gene.25154) and (Gene.22949) could be observed in infected urine. They could be potential biomarkers for Mekongi schistosomiasis diagnosis. Some *S. mekongi* proteins were upregulated in the 2nd, 4th, and 8th weeks but not in the 1st week. This finding may be related to the 1-week incubation periods, during which the schistosomula mature into adult forms without producing eggs [39]. Symptoms typically appear between 2 and 6 weeks after exposure, aligning with the maturation of adult forms, mating, and egg-laying [40]. It has been postulated that the condition is caused by the passage of soluble antigens from the eggs into the bloodstream, resulting in an inflammatory response [41]. The increase in *S. mekongi* proteins found in the urine in the 2nd, 4th, and 8th weeks of exposure might be related to these soluble antigens and the excretory-secretory products from *S. mekongi* eggs.

For *S. mekongi* peptide identification, two peptide sequences derived from collagen alpha-1(V) could be observed at all time points. Collagen is the most abundant protein in the extracellular matrix and the major structure element of connective tissue [42]. Collagen alpha-1(V) is a regulator of collagen fibril formation, matrix assembly, and tissue function [43]. In *S. japonicum*, the collagen alpha-1 (V) chain was among the top 25 genes enriched in cercariae, hepatic schistosomula, mixed adult worms, and eggs [44]. Upon invading a mammalian host, schistosomes have developed intricate mechanisms to adapt to and thrive in the challenging host environment. Notably, they manifest a distinctive syncytial tegument and employ strategies such as antigenic mimicry [45], immune modulation

Table 5
The peptides originating from *S. mekongi*, observed in urine samples from *S. mekongi* infected urine across the 1, 2, 4, and 8-week intervals identified using LC-MS/MS. The red color denotes proteins that are consistently identified in all weeks after infection.

Week	Peptide	Modification	Protein	m/z	Score	e-value	Protein
1st	GEIGPIGMVGVPGQV		Collagen alpha-1(V)	713.3334	36.33	1.50E-01	Gene.3620::comp961_seq0::g.3620::m.3620
	SPGERGPPGIMGAEGQ		Collagen alpha-1(V)	770.355	32.7	3.70E-01	Gene.3620::comp961_seq0::g.3620::m.3620
	GLPGLPGLPGLPGHRGHKG		Collagen alpha-1(V)	909.4	38.1	1.30E-01	Gene.3620::comp961_seq0::g.3620::m.3620
	GEIGPIGMVGVPGQVG		Collagen alpha-1(V)	741.8465	35.6	1.90E-01	Gene.3620::comp961_seq0::g.3620::m.3620
	GLPGLPGLPGLPG		Collagen alpha-1(V)	572.7677	63.79	0.00026	Gene.3620::comp961_seq0::g.3620::m.3620
2nd	ILGGQEAAAHARPYM		Collagen alpha-1(V)	534.2644	57.94	0.0011	Gene.32942::comp54472_seq0::g.32942::m.32942
	ILGGQEAAAHARPYMAS		Collagen alpha-1(V)	586.9568	57.97	0.0012	Gene.32942::comp54472_seq0::g.32942::m.32942
	GLPGLPGLPGLPGHRGHKG		Collagen alpha-1(V)	909.4047	30.86	0.67	Gene.3620::comp961_seq0::g.3620::m.3620
	GLPGLPGLPGLPG		Collagen alpha-1(V)	572.7667	58.01	0.00097	Gene.3620::comp961_seq0::g.3620::m.3620
4th	GEIGPIGMVGVPGQV		Collagen alpha-1(V)	713.3355	41.54	0.046	Gene.3620::comp961_seq0::g.3620::m.3620
	ILGGQEAAAHARPYMAS		Collagen alpha-1(V)	586.9585	63.52	0.00032	Gene.32942::comp54472_seq0::g.32942::m.32942
	GLPGLPGLPGLPGHRGHKG		Collagen alpha-1(V)	909.4058	37.08	0.16	Gene.3620::comp961_seq0::g.3620::m.3620
	GLPGLPGLPGLPG		Collagen alpha-1(V)	572.7685	60.51	0.00054	Gene.3620::comp961_seq0::g.3620::m.3620
8th	GDSGPKGNVGKIGSPGP		Collagen alpha-1(V)	762.3678	35.69	0.18	Gene.3620::comp961_seq0::g.3620::m.3620
	GLPGLPGLPGLPGHRGHKG		Collagen alpha-1(V)	909.6028	36.06	0.21	Gene.3620::comp961_seq0::g.3620::m.3620
	GEIGPIGMVGVPGQVG		Collagen alpha-1(V)	741.8444	33.03	0.34	Gene.3620::comp961_seq0::g.3620::m.3620
	GLPGLPGLPGLPG		Collagen alpha-1(V)	572.7654	60.4	0.00056	Gene.3620::comp961_seq0::g.3620::m.3620
	GEIGPIGMVGVPGQV		Collagen alpha-1(V)	713.3328	41.4	0.048	Gene.3620::comp961_seq0::g.3620::m.3620
	SPGERGPPGIMGAEGQ		Collagen alpha-1(V)	770.3553	33.41	0.32	Gene.3620::comp961_seq0::g.3620::m.3620

	Homo sapiens	*Mus musculus*	*S. mansoni*	*S. mekongi*	*S. japonicum*
Homo sapiens	100.0	100.0	39.0	38.9	39.0
Mus musculus	100.0	100.0	39.0	38.9	39.0
S. mansoni	39.0	39.0	100.0	90.4	91.2
S. mekongi	38.9	38.9	90.4	100.0	97.3
S. japonicum	39.0	39.0	91.2	97.3	100.0

Fig. 6. Percent identity matrix of collagen alpha-1 proteins in *S. makongi*, *S. mansoni*, *S. japonicum*, mouse and human.

[46], and evasion [47,48]. Among extracellular matrix constituents within hepatic schistosomula are collagen components, exemplified by collagen alpha-1(V) chain, alpha-1(IV) chain, alpha-1(XXIV) chain, alpha-2(I) chain, and alpha-2(V) chain. This observation explained the intriguing possibility that collagen components may serve to construct a protective barrier on the worm surface, potentially facilitating schistosomula in evading host immune responses. The identification of elevated expression levels of *S. mekongi* collagen alpha-1(V) in mouse urine suggests a potential association with the heightened synthesis of this protein, contributing to the formation of the worm surface. This phenomenon may also play a role in facilitating host evasion strategies employed by the parasite. The uncharacterized proteins (Gene.25154), (Gene.22949) and collagen alpha-1(V) exhibited notable homology with *Schistosoma* spp., displaying comparatively lower similarity to corresponding proteins in mice and humans. This suggests that uncharacterized proteins (Gene.25154), (Gene.22949) and collagen alpha-1(V) hold promise as a candidate biomarker in the development of *Schistosoma* diagnostic assays, particularly in urine samples.

Based on our results, these protein and peptide biomarkers could be detected by mass spectrometry. However, further validation is

required to assess their sensitivity for antigen-antibody interaction detection. Additionally, validation is needed to confirm the cross-detection of other pathogen infections. The characterization of the identified candidate biomarker within human urine may yield valuable insights, potentially contributing to the early diagnosis of schistosomiasis.

Funding statement

This research project was supported by Mahidol University (Basic Research Fund: fiscal year 2024).

Data availability statement

All the mass spectrometry raw data have been deposited in the Science Data Bank repository, accession number 10.57760/sciencedb.08682 (https://www.scidb.cn/en/anonymous/YlFCZmlt).

Additional information

No additional information is available for this paper.

CRediT authorship contribution statement

Tipparat Thiangtrongjit: Writing – review & editing, Writing – original draft, Methodology, Formal analysis. **Poom Adisakwattana:** Writing – review & editing, Writing – original draft, Investigation, Formal analysis, Conceptualization. **Yanin Limpanont:** Resources, Methodology. **Wang Nguitragool:** Writing – review & editing, Writing – original draft, Supervision, Funding acquisition, Conceptualization. **Phiraphol Chusongsang:** Resources. **Yupa Chusongsang:** Resources. **Nuttapohn Kiangkoo:** Resources. **Onrapak Reamtong:** Writing – review & editing, Writing – original draft, Supervision, Methodology, Investigation, Formal analysis, Conceptualization.

Declaration of competing interest

The authors declare that they have no known competing financial interests or personal relationships that could have appeared to influence the work reported in this paper.

Acknowledgment

The authors would like to thank the Tropical Medicine Diagnostic Development Unit for technical support and assistance in the experiment of this study.

Appendix A. Supplementary data

Supplementary data to this article can be found online at https://doi.org/10.1016/j.heliyon.2024.e35439.

References

[1] B. Chala, Advances in diagnosis of Schistosomiasis: focus on challenges and future approaches, Int. J. Gen. Med. 16 (2023) 983–995.
[2] B. Gryseels, K. Polman, J. Clerinx, L. Kestens, Human schistosomiasis, Lancet 368 (9541) (2006) 1106–1118.
[3] S. Muth, S. Sayasone, S. Odermatt-Biays, S. Phompida, S. Duong, P. Odermatt, *Schistosoma mekongi* in Cambodia and Lao people's democratic republic, Adv. Parasitol. 72 (2010) 179–203.
[4] C. Urbani, M. Sinoun, D. Socheat, K. Pholsena, H. Strandgaard, P. Odermatt, C. Hatz, Epidemiology and control of Mekong schistosomiasis, Acta Trop. 82 (2) (2002) 157–168.
[5] D.P. McManus, D.W. Dunne, M. Sacko, J. Utzinger, B.J. Vennervald, X.N. Zhou, Schistosomiasis, Nat Rev Dis Primers 4 (1) (2018) 13.
[6] D.J. Gray, A.G. Ross, Y.S. Li, D.P. McManus, Diagnosis and management of schistosomiasis, BMJ 342 (2011) d2651.
[7] R. Rodpai, L. Sadaow, O. Sanpool, P. Boonroumkaew, T. Thanchomnang, S. Laymanivong, P. Janwan, Y. Limpanont, P. Chusongsang, H. Ohmae, H. Yamasaki, Z. Lv, P.M. Intapan, W. Maleewong, Development and accuracy evaluation of lateral flow immunoassay for rapid diagnosis of schistosomiasis mekongi in Humans, Vector Borne Zoonotic Dis. 22 (1) (2022) 48–54.
[8] B. Nickel, S. Sayasone, Y. Vonghachack, P. Odermatt, H. Marti, *Schistosoma mansoni* antigen detects *Schistosoma mekongi* infection, Acta Trop. 141 (Pt B) (2015) 310–314.
[9] J.M.M. Angeles, A. Wanlop, M.A. Dang-Trinh, M. Kirinoki, S.I. Kawazu, A. Yajima, Evaluation of crude and recombinant antigens of *Schistosoma japonicum* for the detection of *Schistosoma mekongi* human infection, Diagnostics 13 (2) (2023) 184.
[10] Y. Zhu, W. Hua, M. Xu, W. He, X. Wang, Y. Dai, S. Zhao, J. Tang, S. Wang, S. Lu, A novel immunodiagnostic assay to detect serum antibody response against selected soluble egg antigen fractions from *Schistosoma japonicum*, PLoS One 7 (8) (2012) e44032.
[11] N. Kato-Hayashi, M. Kirinoki, Y. Iwamura, T. Kanazawa, V. Kitikoon, H. Matsuda, Y. Chigusa, Identification and differentiation of human schistosomes by polymerase chain reaction, Exp. Parasitol. 124 (3) (2010) 325–329.
[12] O. Sanpool, P.M. Intapan, T. Thanchomnang, P. Sri-Aroon, V. Lulitanond, L. Sadaow, W. Maleewong, Development of a real-time PCR assay with fluorophore-labelled hybridization probes for detection of *Schistosoma mekongi* in infected snails and rat feces, Parasitology 139 (10) (2012) 1266–1272.

[13] K.G. Weerakoon, G.N. Gobert, P. Cai, D.P. McManus, Advances in the Diagnosis of human schistosomiasis, Clin. Microbiol. Rev. 28 (4) (2015) 939–967.
[14] D.G. Colley, W.E. Secor, Immunology of human schistosomiasis, Parasite Immunol. 36 (8) (2014) 347–357.
[15] V. Silva-Moraes, J.M. Ferreira, P.M. Coelho, R.F. Grenfell, Biomarkers for schistosomiasis: towards an integrative view of the search for an effective diagnosis, Acta Trop. 132 (2014) 75–79.
[16] Y. Hong, A. Sun, M. Zhang, F. Gao, Y. Han, Z. Fu, Y. Shi, J. Lin, Proteomics analysis of differentially expressed proteins in schistosomula and adult worms of *Schistosoma japonicum*, Acta Trop. 126 (1) (2013) 1–10.
[17] N. Amiri-Dashatan, M. Koushki, H.A. Abbaszadeh, M. Rostami-Nejad, M. Rezaei-Tavirani, Proteomics applications in health: biomarker and drug discovery and food industry, Iran. J. Pharm. Res. (IJPR) 17 (4) (2018) 1523–1536.
[18] J. Archer, J.E. LaCourse, B.L. Webster, J.R. Stothard, An update on non-invasive urine diagnostics for human-infecting parasitic helminths: what more could be done and how? Parasitology 147 (8) (2020) 873–888.
[19] T. Thiangtrongjit, P. Adisakwattana, Y. Limpanont, P. Dekumyoy, S. Nuamtanong, P. Chusongsang, Y. Chusongsang, O. Reamtong, Proteomic and immunomic analysis of *Schistosoma mekongi* egg proteins, Exp. Parasitol. 191 (2018) 88–96.
[20] O. Reamtong, N. Simanon, T. Thiangtrongjit, Y. Limpanont, P. Chusongsang, Y. Chusongsang, S. Anuntakarun, S. Payungporn, O. Phuphisut, P. Adisakwattana, Proteomic analysis of adult *Schistosoma mekongi* somatic and excretory-secretory proteins, Acta Trop. 202 (2020) 105247.
[21] O. Phuphisut, P. Ajawatanawong, Y. Limpanont, O. Reamtong, S. Nuamtanong, S. Ampawong, S. Chaimon, P. Dekumyoy, D. Watthanakulpanich, B. E. Swierczewski, P. Adisakwattana, Transcriptomic analysis of male and female *Schistosoma mekongi* adult worms, Parasites Vectors 11 (2018) 504.
[22] Y. Ishihama, Y. Oda, T. Tabata, T. Sato, T. Nagasu, J. Rappsilber, M. Mann, Exponentially modified protein abundance index (emPAI) for estimation of absolute protein amount in proteomics by the number of sequenced peptides per protein, Mol. Cell. Proteomics 4 (2005) 1265–1272.
[23] O.S. Onile, B. Calder, N.C. Soares, C.I. Anumudu, J.M. Blackburn, Quantitative label-free proteomic analysis of human urine to identify novel candidate protein biomarkers for schistosomiasis, PLoS Neglected Trop. Dis. 11 (11) (2017) e0006045.
[24] P. Makhijani, P.J. Basso, Y.T. Chan, N. Chen, J. Baechle, S. Khan, D. Furman, S. Tsai, D.A. Winer, Regulation of the immune system by the insulin receptor in health and disease, Front. Endocrinol. 14 (2023) 1128622.
[25] Y. Zhou, L. Rui, Major urinary protein regulation of chemical communication and nutrient metabolism, Vitam Horm 83 (2010) 151–163.
[26] C.S. Forster, K. Johnson, V. Patel, R. Wax, N. Rodig, J. Barasch, R. Bachur, R.S. Lee, Urinary NGAL deficiency in recurrent urinary tract infections, Pediatr. Nephrol. 32 (6) (2017) 1077–1080.
[27] J. Barratt, I. Weitz, Complement Factor D as a strategic target for regulating the alternative complement pathway, Front. Immunol. 12 (2021) 712572.
[28] J.R. Dunkelberger, W.C. Song, Complement and its role in innate and adaptive immune responses, Cell Res. 20 (1) (2010) 34–50.
[29] F. Zeng, R.C. Harris, Epidermal growth factor, from gene organization to bedside, Semin. Cell Dev. Biol. 28 (2014) 2–11.
[30] M. Simanski, F. Rademacher, L. Schröder, R. Gläser, J. Harder, The inflammasome and the epidermal growth factor receptor (EGFR) are involved in the *Staphylococcus aureus*-mediated induction of IL-1alpha and IL-1beta in human keratinocytes, PLoS One 11 (1) (2016) e0147118.
[31] J. Chao, L. Chao, Kallikrein-kinin in stroke, cardiovascular and renal disease, Exp. Physiol. 90 (3) (2005) 291–298.
[32] S. Marcondes, E. Antunes, The plasma and tissue kininogen-kallikrein-kinin system: role in the cardiovascular system, Curr. Med. Chem. Cardiovasc. Hematol. Agents 3 (1) (2005) 33–44.
[33] J. Scharfstein, D. Andrade, E. Svensjö, A.C. Oliveira, C.R. Nascimento, The kallikrein-kinin system in experimental Chagas disease: a paradigm to investigate the impact of inflammatory edema on GPCR-mediated pathways of host cell invasion by *Trypanosoma cruzi*, Front. Immunol. 3 (2013) 396.
[34] R. Immler, B. Lange-Sperandio, T. Steffen, H. Beck, I. Rohwedder, J. Roth, M. Napoli, G. Hupel, F. Pfister, B. Popper, B. Uhl, H. Mannell, C.A. Reichel, V. Vielhauer, J. Scherberich, M. Sperandio, M. Pruenster, Extratubular polymerized uromodulin induces leukocyte recruitment and inflammation in vivo, Front. Immunol. 11 (2020) 588245.
[35] R.L.F. Galvao, G.C. Meneses, M.C.C. Pinheiro, A.M.C. Martins, E.F. Daher, F.S.M. Bezerra, Kidney injury biomarkers and parasitic loads of *Schistosoma mansoni* in a highly endemic area in northeastern Brazil, Acta Trop. 228 (2022) 106311.
[36] Z. Wu, Z. Zhang, Z. Lei, P. Lei, CD14: biology and role in the pathogenesis of disease, Cytokine Growth Factor Rev. 48 (2019) 24–31.
[37] M.Y. Lee, C.H. Huang, C.J. Kuo, C.L. Lin, W.T. Lai, S.H. Chiou, Clinical proteomics identifies urinary CD14 as a potential biomarker for diagnosis of stable coronary artery disease, PLoS One 10 (2) (2015) e0117169.
[38] K.Y. Lee, Y.L. Lee, M.H. Chiang, H.Y. Wang, C.Y. Chen, C.H. Lin, Y.C. Chen, C.K. Fan, P.C. Cheng, *Schistosoma* egg antigens suppress LPS-induced inflammation in human IMR-90 cells by modulation of JAK/STAT1 signaling, J. Microbiol. Immunol. Infect. 54 (3) (2021) 501–513.
[39] E. Bottieau, J. Clerinx, M.R. de Vega, E.V. den Enden, R. Colebunders, M. Van Esbroeck, T. Vervoort, A. Van Gompel, J.V.D. Ende, Imported Katayama fever: clinical and biological features at presentation and during treatment, J. Infect. 52 (2006) 339–345.
[40] S. Jauréguiberry, L. Paris, E. Caumes, Acute schistosomiasis, a diagnostic and therapeutic challenge, Clin. Microbiol. Infect. 16 (2010) 225–231.
[41] C. Carbonell, B. Rodríguez-Alonso, A. López-Bernús, H. Almeida, I. Galindo-Pérez, V. Velasco-Tirado, M. Marcos, J. Pardo-Lledías, M. Belhassen-García, Clinical spectrum of schistosomiasis: an update, J. Clin. Med. 10 (23) (2021) 5521.
[42] K. Gelse, E. Pöschl, T. Aigner, Collagens-structure, function, and biosynthesis, Adv. Drug Deliv. Rev. 55 (12) (2003) 1531–1546.
[43] M. Sun, S. Chen, S.M. Adams, J.B. Florer, H. Liu, W.W. Kao, R.J. Wenstrup, D.E. Birk, Collagen V is a dominant regulator of collagen fibrillogenesis: dysfunctional regulation of structure and function in a corneal-stroma-specific Col5a1-null mouse model, J. Cell Sci. 124 (Pt 23) (2011) 4096–4105.
[44] P. Cai, S. Liu, X. Piao, N. Hou, H. You, D.P. McManus, Q. Chen, A next-generation microarray further reveals stage-enriched gene expression pattern in the blood fluke *Schistosoma japonicum*, Parasites Vectors 10 (1) (2017) 19.
[45] C. Wu, N. Hou, X. Piao, S. Liu, P. Cai, Y. Xiao, Q. Chen, Non-immune immunoglobulins shield *Schistosoma japonicum* from host immunorecognition, Sci. Rep. 5 (2015) 13434.
[46] S.J. Jenkins, J.P. Hewitson, G.R. Jenkins, A.P. Mountford, Modulation of the host's immune response by schistosome larvae, Parasite Immunol. 27 (10–11) (2005) 385–393.
[47] P. Cai, L. Bu, J. Wang, Z. Wang, X. Zhong, H. Wang, Molecular characterization of *Schistosoma japonicum* tegument protein tetraspanin-2: sequence variation and possible implications for immune evasion, Biochem. Biophys. Res. Commun. 372 (1) (2008) 197–202.
[48] W. Zhang, J. Li, M. Duke, M.K. Jones, L. Kuang, J. Zhang, D. Blair, Y. Li, D.P. McManus, Inconsistent protective efficacy and marked polymorphism limits the value of *Schistosoma japonicum* tetraspanin-2 as a vaccine target, PLoS Neglected Trop. Dis. 5 (5) (2011) e1166.